Predicting Loess Collapsibility Using Grey Relational Analysis and Transformer Networks

Zeliang Chen
Lanzhou New Area Urban Construction Engineering Co., Ltd., Lanzhou 73000, China
E-mail: czlchen@inap.ac.cn

Keywords: Loess, transformer network, grey relational degree, collapsibility indicators, prediction model

Received: January 22, 2026

Subgrade and pavement diseases caused by loess collapsibility seriously affect the safety and durability of road engineering. Precise prediction of the collapsibility coefficient plays a pivotal role in engineering prevention and control in loess regions. To address the issues where loess collapsibility is influenced by the coupling effect of multiple factors and traditional forecasting approaches lack adequate generalization capability, this study presents a predictive model integrating grey relational analysis and Transformer network, based on the NCE7# Highway project in Lanzhou New Area. Firstly, indoor experiments were conducted to analyze the correlation between various indicators (such as sampling depth and compaction state) and the collapsibility coefficient. Grey relational degree was used to screen out saturation (0.79), natural density (0.78), void ratio (0.71), and compression coefficient (0.71) as core indicators, eliminating weakly correlated redundant information. Subsequently, an optimized Transformer model was constructed based on these core indicators, which captures the deep coupling relationships among indicators through the self-attention mechanism. Based on indoor experimental data, comparative verification was carried out with RF, BP, and SVM models. The results demonstrate that the Transformer model achieves an R^2 of 0.976 and an MSE of 0.0009 on the training set, and an R^2 of 0.953 and an MSE of 0.0015 on the test set. Compared with traditional models, the MSE is reduced by 57.1% – 67.9% and the R^2 is improved by 5.7% – 8.9%. The model stabilizes after only 42 epochs, with a generalization performance decay of merely 8.3%, significantly outperforming the decay rate of over 35% observed in traditional models, effectively mitigating the overfitting problem. In summary, this study accurately screens core indicators through grey relational degree and combines the powerful feature extraction capability of the Transformer network to realize high-precision and stable prediction of the loess collapsibility coefficient. It provides a scientific basis and efficient technical support for the formulation of foundation treatment schemes, disease prevention and control, and service life extension of road engineering in loess areas.

Povzetek: Študija predlaga napoved koeficienta sesedljivosti lesa, ki z metodo sive relacijske analize izbere ključne geotehnične kazalnike ter jih nato modelira z optimiziranim Transformerjem za zajem nelinearnih sklopitev in boljšo posplošitev kot klasični RF/BP/SVM.

1 Introduction

During the construction and service phases of highways in loess regions, collapsible loess tends to undergo sudden structural collapse and volume shrinkage upon water immersion, resulting in a range of engineering defects including subgrade uneven settlement, pavement cracking, void development, and pumping phenomena. These issues seriously threaten driving safety and reduce road durability [1,2]. As the core indicator for quantifying the degree of loess collapsibility, the collapsibility coefficient is not only an important basis for classifying collapsibility grades and determining foundation treatment schemes, but its accurate prediction is also a key prerequisite for realizing prospective prevention and control of engineering diseases [3,4].

One of the core research directions in the mechanism of loess collapsibility is the accurate identification of key soil properties that regulate collapsibility, and numerous scholars have carried out systematic research around this direction. Shu et al. [5] conducted indoor experiments by adjusting loess moisture content, combined with multivariate statistical analysis methods, constructed a binary regression model of initial moisture content, initial void ratio and collapsibility coefficient, and clarified the quantitative correlation among the three; Zheng et al. [6] used microscopic testing technology to deeply analyze the intrinsic correlation between loess moisture content and mechanical properties, providing microscopic support for revealing the regulatory mechanism of moisture state on collapsibility; Zhu et al. [7] systematically analyzed the correlation between collapsibility coefficient and various soil properties using mathematical statistics methods, and performed dimensionality reduction and screening of loess physical parameters combined with factor analysis theory; Lv et al. [8] focused on the correlation law between collapsibility and moisture content through

mathematical statistics, and simultaneously explored the coupling relationship between collapsibility coefficient and other key physical indicators.

The prediction methods of loess collapsibility coefficient have gradually evolved from traditional empirical formula methods to data-driven model systems. In recent years, machine learning models have become the mainstream research direction in this field due to their powerful nonlinear fitting capabilities [9,10]. Zhao et al. [11] developed a support vector machine (SVM) prediction model founded on a statistical learning framework to classify the collapsibility degree of loess in Xining City, offering a basis for the assessment of regional loess collapsibility; Ren et al. [12] integrated various data mining technologies to construct a combined prediction model of discrete binomial coefficients for loess collapsibility, showing good prediction results; Guo et al. [13] established a loess collapsibility prediction model integrating PLS method and Logistic Cum function based on existing experimental data, improving the adaptability of the prediction method; Chen et al. [14] established a multiple linear regression model to predict the collapsibility coefficient of loess in Xinyuan County, explicitly quantifying the linear correlation between the collapsibility coefficient and diverse impact factors. Overall, existing prediction models still have obvious limitations: first, they insufficiently capture the deep nonlinear coupling relationships among multiple soil properties, making it difficult to adapt to the complex nature of loess collapsibility affected by the synergistic effect of multiple factors; second, under the condition of small sample data common in engineering scenarios, the model generalization performance degrades significantly, and the overfitting problem is prominent; third, some models have slow convergence rates, and the training efficiency is difficult to meet the needs of rapid decision-making in practical engineering. Therefore, developing an integrated prediction model with "accurate indicator screening - strong feature extraction - high generalization stability" has become a core research gap in the current field of loess collapsibility coefficient prediction.

To this end, this study takes the collapsible loess road project of NCE7# Road (Weier Shisan Road ~ Weier Shijiu Road) in Lanzhou New Area as the research carrier, and proposes a loess collapsibility coefficient prediction model integrating grey relational degree and Transformer network. Firstly, indoor experiments are conducted to systematically obtain measured data of various soil properties and collapsibility coefficients. Grey relational degree analysis is used to quantify the correlation strength between each indicator and the collapsibility coefficient, accurately screening out the core indicators that dominate collapsibility and eliminating weakly correlated and redundant information. Subsequently, an optimized Transformer network model is constructed based on the core indicators, and the self-attention mechanism is used to capture the global dependencies and deep coupling relationships among indicators, breaking through the feature representation limitations of traditional models. Finally, through comparative verification with traditional models such as RF, BP, and SVM, the fitting accuracy, convergence efficiency, and generalization performance of the proposed model are systematically evaluated. This study aims to address the following three core issues: (1) accurately identifying the key indicators that dominate loess collapsibility from a multi-factor coupled loess index system; (2) overcoming the limitations of traditional models regarding overfitting with small-sample data, and constructing a prediction model that possesses both high fitting accuracy and strong generalization capability; and (3) establishing a closed-loop decision-making mechanism from collapsibility prediction to engineering control.

2 Engineering overview and loess collapsibility test analysis

2.1 Engineering overview and quantitative characterization of loess collapsibility

The NCE7# Road project (Weier Shisan Road ~ Weier Shijiu Road) in Lanzhou New Area has a total length of 2371.95 m, including a reconstructed section of 492.37 m and a newly built section of 1879.57 m. It is located in the southern area of Lanzhou New Area (southwest of Xicha Town, Gaolan County, Lanzhou City). From the perspective of geomorphic division, the entire road is situated in the loess hills and valley areas in the southeast of the Qinwangchuan Basin, belonging to a denudational accumulative hilly landform, with microgeomorphic units of loess ridges, hills, and gullies. According to the geological survey report, the soil layers along the road exhibit Grade IV (very severe) self-weight collapsibility. The loess in this region is mostly underconsolidated structured soil, with particles bonded by cementing substances such as carbonates, forming a honeycomb pore structure. During the construction and operation of the subgrade and pavement, when the soil encounters water, the cementing substances dissolve, the interparticle bonding force is lost, the honeycomb structure collapses, and the soil volume shrinks sharply with additional settlement. Notably, such settlement is characterized by suddenness and unevenness. As shown in Figure 1, when the loess settles due to collapsibility, the subgrade is prone to unequal settlement deformation, which further leads to pavement diseases including unequal subsidence, continuous cracks, local voids and pumping, and sinkhole collapse, damaging the structural integrity and flatness of the pavement. If these diseases persist, they will reduce driving comfort and safety, shorten the service life of the road, and increase later maintenance costs [15-17].

Figure 1: Road diseases caused by loess collapsibility

To quantitatively characterize the degree of loess collapsibility, commonly used methods in engineering mainly include collapsibility coefficient, initial collapsibility pressure, collapsibility grade, relative collapsibility amount, and difference in compression coefficient. The initial collapsibility pressure is used to characterize the critical stress condition for loess to undergo collapsibility, defining the stress threshold for collapsible deformation of loess. The collapsibility grade is a systematic evaluation result integrating multiple parameters such as collapsibility coefficient and collapsible thickness, reflecting the overall severity of loess collapsibility hazards. The relative collapsibility amount focuses on quantifying the relative scale of collapsible deformation, intuitively demonstrating the macro impact range of collapsible deformation. The difference in compression coefficient can only indirectly reflect the change law of loess compression characteristics before and after collapsibility, and cannot directly characterize the essence of collapsibility intensity. Since the collapsibility coefficient can directly quantify the additional deformation of loess when encountering water under a specific pressure through mature indoor oedometer tests, it accurately reflects the essential characteristics of loess collapsibility intensity. Meanwhile, as the core basic parameter for classifying loess collapsibility types and determining collapsibility grades, this indicator can provide key quantitative basis for the formulation of engineering foundation treatment schemes. Based on this, the collapsibility coefficient is selected as the preferred indicator for characterizing loess collapsibility in this study.

2.2 Correlation analysis between loess collapsibility and various indicators

Loess collapsibility is a product of the synergistic effect of external environmental factors such as external loads and moisture content changes, and internal properties such as granular honeycomb microstructure. The intensity of loess collapsibility can be quantitatively depicted by the collapsibility coefficient. To systematically explore the mechanism through which each impact factor acts on loess collapsibility, this study selects loess samples from the NCE7# Highway project (Weier Shisan Road ~ Weier Shijiu Road) in Lanzhou New Area as the research subject, carries out indoor collapsibility tests, and adopts the control variable method to quantitatively analyze the influence regularity of various factors on loess collapsibility.

(1) Correlation between sampling depth and collapsibility coefficient:

Depth is a macro dominant factor affecting loess collapsibility. It regulates the microstructures of loess by changing the overlying load intensity, thereby affecting the collapsibility coefficient. The correlation between the collapsibility coefficient of the tested loess samples and sampling depth is illustrated in Figure 1. As depicted in Figure 2, the collapsibility coefficient exhibits a distinct negative correlation with sampling depth. In the study area, the termination depth of loess collapsibility is approximately 25 m, while the initial depth of strong collapsibility is roughly 9 m. That is, the distribution range of collapsible loess is within 25 m, and severely collapsible loess is concentrated within 9 m. This depth dependence is essentially the result of the superposition of pore structure evolution and load action, providing a macro basis for conducting collapsibility evaluation by depth.

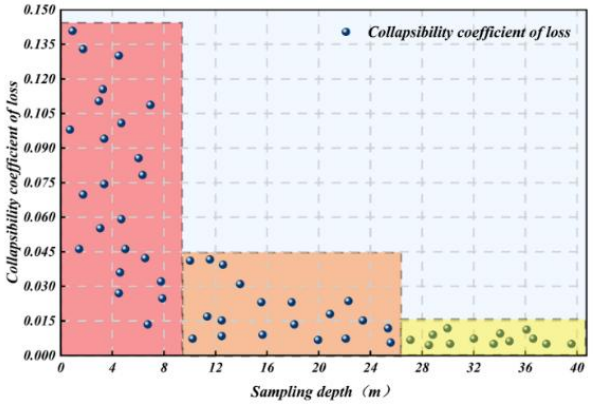

Figure 2: Correlation between sampling depth and collapsibility coefficient

(2) Correlation Between Compactness Indicators and Collapsibility Coefficient

Compactness indices (natural density, dry density) directly govern loess collapsibility intensity through reflecting the compactness of the soil particle framework, and both exhibit a significant negative correlation with the collapsibility coefficient. As illustrated in Figure 3, when the dry density exceeds 1.61 g/cm³, the loess is non-collapsible; when it is below 1.30 g/cm³, the loess exhibits mainly moderate to severe collapsibility. This is primarily due to the fact that the lower the dry density, the fewer the particles per unit volume and the looser the soil skeleton. When immersed in water or disturbed by external forces, the soil's particle arrangement and bonding properties are liable to undergo drastic alterations, thereby leading to enhanced collapsibility. The negative correlation between natural density and the collapsibility coefficient aligns with that between dry density and the coefficient: when the natural density is above 1.95 g/cm³, the loess exhibits no collapsibility; when it is below 1.50 g/cm³, it falls into the range of strong collapsibility.

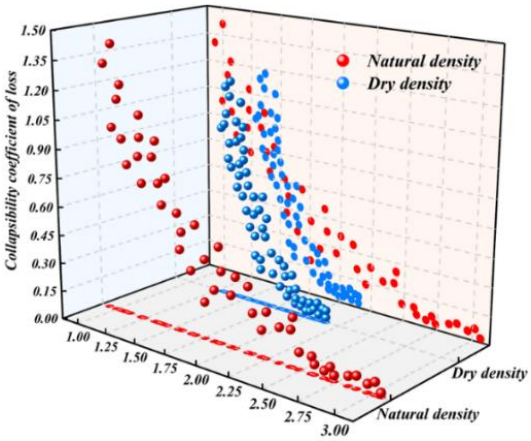

Figure 3: Correlation between compactness indicators and collapsibility coefficient

(3) Correlation between pore structure indices and collapsibility coefficient:

Pore structure is the core internal factor of loess collapsibility. Indices such as void ratio and porosity directly determine the spatial potential for collapsible deformation by characterizing the proportion of pore volume. As shown in Figure 4, both void ratio and porosity show a significant positive correlation with the collapsibility coefficient. Loess exhibits obvious collapsibility when the porosity ranges from 38% to 55% and the void ratio ranges from 0.824 to 1.239; when the porosity is less than 31% and the void ratio is less than 0.712, loess generally does not have collapsibility. This is mainly because the void ratio and porosity directly reflect the enrichment degree of vuggy pores. The larger their values, the more sufficient the compressible deformation space inside the soil mass; after water immersion, the amplitude of particle sliding and pore collapse is greater, leading to stronger collapsibility.

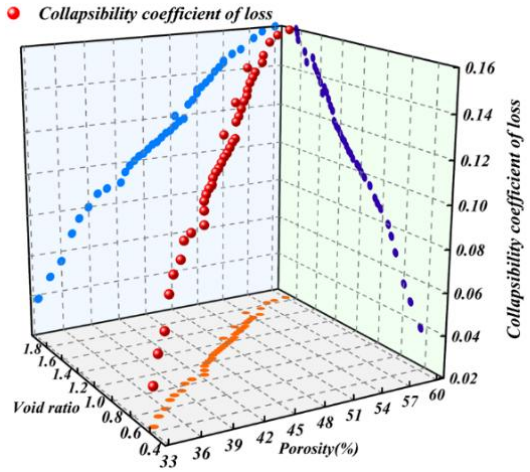

Figure 4: Correlation between pore structure indices and collapsibility coefficient

(4) Correlation between water content state indicators and collapsibility coefficient

The "water sensitivity" of loess dictates that water content state indices (natural water content, degree of saturation) exert a notable regulatory role on the collapsibility coefficient. As demonstrated in Figure 5, although a certain degree of scatter exists between natural water content and the collapsibility coefficient, they still display an overall significant negative correlation; by comparison, the negative correlation between the collapsibility coefficient and degree of saturation is more pronounced, with a correlation strength higher than that between the collapsibility coefficient and natural water content. The collapsibility coefficient exhibits a declining trend as the initial natural water content and degree of saturation increase. When both rise to specific thresholds—specifically, when the natural water content and degree of saturation of the loess exceed 25% and 63%, respectively—the collapsibility coefficient will be below 0.015, and no collapsible deformation takes place. Furthermore, when the initial natural water content of the loess is below 12% and the initial degree of saturation is below 39%, the loess is predominantly characterized by strong collapsibility.

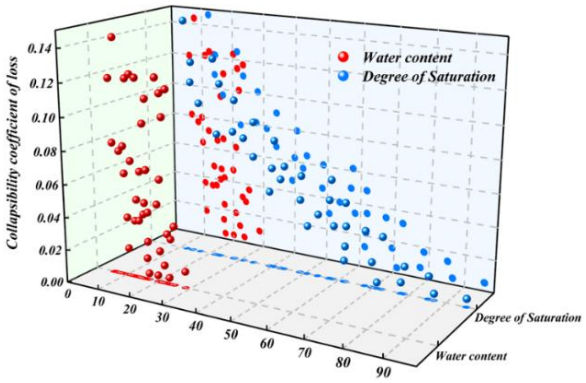

Figure 5: Correlation between water content state indicators and collapsibility coefficient

In addition, as a core parameter characterizing the soil consistency state, the liquidity index (IL) can not only accurately judge the hardness and softness of the soil but also comprehensively reflect its particle composition and humidity characteristics, serving as a relative index for characterizing the soil water content state (Table 1). Unlike direct indicators quantifying the absolute water content such as natural water content and degree of saturation, the liquidity index quantifies the relative position of the natural water content within the plastic range through normalized comparison between the soil's natural water content and its own liquid limit and plastic limit, thereby more objectively revealing the relative saturation degree of the soil's water content state. When the liquidity index is small (IL < 0, in the hard state), the natural water content of loess is lower than the plastic limit, and the skeleton structure is in a stable underconsolidated state. However, at this time, large pores develop inside the soil with good connectivity; after water immersion, the cementing materials soften rapidly, particles lose support, and significant collapsible deformation is prone to occur, resulting in a relatively large collapsibility coefficient. With the increase of the liquidity index, the natural water content rises to between the plastic limit and liquid limit, the cementing materials

have been partially softened, the interparticle bonding force is weakened, the soil has undergone a certain degree of compression in the natural state, the underconsolidation decreases, and the collapsible potential after water immersion is correspondingly reduced.

Table 1: Relationship between soil liquidity index and soil plastic form

Liquidity Index (Ip)	<0	0-0.25	0.25-0.75	0.75-1	>1
Soil Form	Hard	Stiff Plastic	Plastic	Soft Plastic	Flow Plastic

(5) Correlation between Mechanical Indicators and Collapsibility Coefficient

Mechanical parameters such as compression modulus and compression coefficient are key indicators characterizing the compressive deformation behavior of soil. They can quantify the soil's mechanical capacity to resist compressive deformation and have an indirect correlation with the collapsibility coefficient of loess. As presented in Figure 6, the collapsibility coefficient demonstrates a strong positive correlation with the compression coefficient, whereas it typically exhibits a negative correlation with the compression modulus. Loess presents significant collapsibility when the compression coefficient is greater than 0.72 MPa^{-1} and the compression modulus is less than 2.6 MPa; when the compression coefficient is less than 0.19 MPa^{-1} and the compression modulus is greater than 10.6 MPa, loess usually does not possess collapsibility. This is mainly because the higher the compression modulus and the lower the compression coefficient, the more stable the internal structure of the soil mass, making it more difficult for plastic deformation and collapsibility to occur after water immersion. On the contrary, soil with a low compression modulus is prone to plastic flow, and its collapsibility is more prominent.

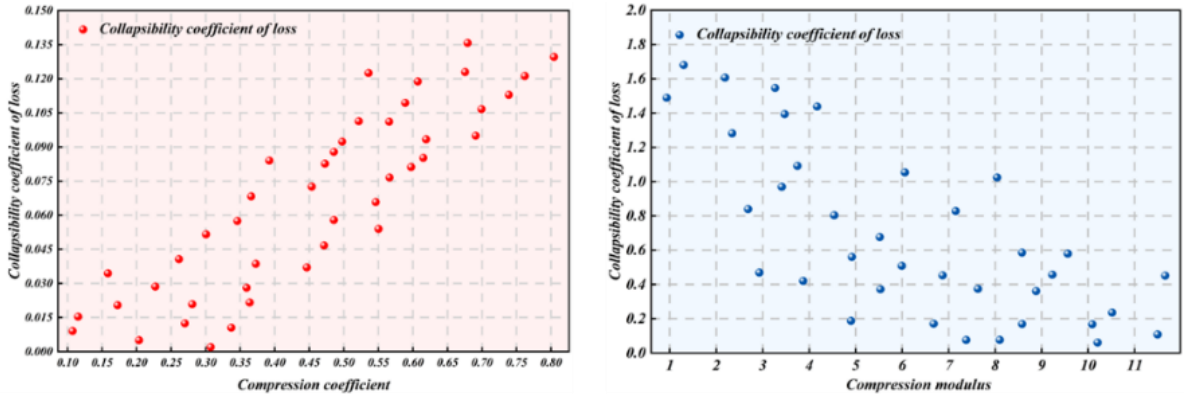

a, Compression coefficient b, Compression modulus

Figure 6: Correlation between mechanical indicators and collapsibility coefficient (a, compression coefficient; b, compression modulus)

3 Loess collapsibility coefficient prediction model based on grey relational analysis and transformer network

3.1 Selection of loess collapsibility indicators based on grey relational analysis

The core prerequisite for predicting the loess collapsibility coefficient resides in precisely identifying the soil properties that dominate loess collapsibility. Given that loess collapsibility is subject to the combined effects of multiple factors (including dry density, natural water content, void ratio, and liquid limit), the correlation mechanism between each index and the collapsibility coefficient is intricate, and certain influencing factors exhibit uncertainties. Traditional single-factor analysis methods are difficult to fully reveal the inherent correlation laws between indicators. Therefore, based on the measured data of loess soil properties and collapsibility coefficients obtained from laboratory tests, this chapter introduces the grey relational analysis method to systematically analyze the correlation characteristics between each soil property index and the collapsibility coefficient, screen out the core indicators that have a significant impact on loess collapsibility, and provide theoretical basis and data support for constructing a high-precision loess collapsibility coefficient prediction model.

Combined with the research scenario of loess collapsibility, the grey relational analysis needs to be carried out in an orderly manner through the following four steps. The core idea is to take the collapsibility coefficient as the core evaluation index (reference sequence) and each soil property index as the influencing factor (comparison sequence), and realize the screening of key influencing indicators by quantifying the correlation degree between the two [18-21].

(1) Determine the reference sequence and comparison sequences

The reference sequence is the sequence reflecting the core behavioral characteristics of loess collapsibility, i.e., the sequence of collapsibility coefficients measured in laboratory tests. If n groups of loess samples are

obtained in total, the reference sequence can be expressed as:

$$A_0 = [A_0(1), A_0(2), \ldots, A_0(n)] \quad (1)$$

Among them, $A_0(k)$（k=1,2,3…,n) represents the collapsibility coefficient value of the k^{th} group of loess samples.

The comparison sequences refer to the sequences of various soil property indicators that affect loess collapsibility. Based on literature review and experimental feasibility, m key soil property indicators including dry density, natural water content, void ratio, plastic limit, and degree of saturation are selected as the comparison sequences. Each comparison sequence corresponds to the measured indicator values of n groups of samples, which can be expressed as:

$$A_i = [A_i(1), A_i(2), \ldots, A_i(n)] \quad (2)$$

Among them, $A_i(k)\,(i = 1,2,\ldots,m\ )$ (i=1,2,3…,m) (k=1,2,…,n)) represents the measured value of the i^{th} soil property indicator for the k^{th} group of loess samples.

(2) Dimensionless Processing of Data

There are significant differences in the dimensions of indicators related to loess collapsibility. Direct analysis will lead to result deviations due to the dimensional effect. Therefore, it is necessary to perform dimensionless processing on the reference sequence and comparison sequences, normalizing all indicator values to the interval [0,1] to eliminate the interference of numerical scale differences on the correlation degree calculation. Combined with the physical significance of loess soil property indicators, different normalization formulas are adopted according to the indicator types (positive, negative, moderate), and the processed indicator is denoted as $A_i'(k)$:

Positive indicators: The larger the indicator value, the weaker the loess collapsibility (e.g., dry density, natural water content). The processing formula is:

$$A_i'(k) = \frac{A_i(k) - min(A_i(k))}{max(A_i(k)) - min(A_i(k))} \quad (3)$$

Negative indicators: The larger the indicator value, the stronger the loess collapsibility (e.g., void ratio, porosity). The processing formula is:

$$A_i'(k) = \frac{max(A_i(k)) - A_i(k)}{max(A_i(k)) - min(A_i(k))} \quad (4)$$

In the formula, $(max(A_i(k))$、$(min(A_i(k))$ represent the maximum and minimum values of the i^{th} indicator, respectively.

(3) Calculate the Relational Coefficients

First, calculate the differences between the reference sequence and each comparison sequence, and then construct the difference sequence $\Delta_i(k)$; subsequently, screen out the minimum difference a and maximum difference b from all difference sequences; finally, calculate the relational coefficient $\gamma_i(k)$ between the reference sequence and each comparison sequence at each moment. The specific calculation formulas are as follows:

$$\Delta_i(k) = |A_0'(k) - A_i'(k)| \quad (i = 1,2,\ldots,m; k = 1,2,\ldots,n) \quad (5)$$

$$a = min_{i,k}\,\Delta_i(k) \quad (6)$$

$$b = max_{i,k}\,\Delta_i(k) \quad (7)$$

$$\gamma_i(k) = \frac{a + \rho b}{\Delta_i(k) + \rho b} \quad (8)$$

Among them, the distinguishing coefficient p is an adjustable parameter with a value range of (0,1), and the conventional value is 0.5.

(4) Calculate and rank the overall relational degrees

A single relational coefficient only reflects local correlation characteristics. It is necessary to integrate the relational coefficients to obtain the overall relational degree that reflects the overall correlation between a certain soil property indicator and the collapsibility coefficient γ_i .The arithmetic mean method is adopted to integrate the relational coefficients: the overall relational degree between the comparison sequence and the reference sequence can be obtained by directly taking the average of the relational coefficients at each moment. The specific formula is as follows:

$$\gamma_i = \frac{1}{n}\sum_{k=1}^{n}\gamma_i(k) \quad (9)$$

In the formula, $\gamma_i \in (0,1]$, the larger (representing the grey relational degree) is, the higher the overall correlation degree between the soil property indicator and loess collapsibility, and the more significant its dominant effect on collapsibility.

Finally, the relational degrees of all comparison sequences are sorted in descending order to form a relational order. The relationship hierarchy directly denotes the priority of influence of each soil property index on loess collapsibility. Based on this, core influencing indicators with high relational degrees can be screened out, and secondary indicators with weak relational degrees can be eliminated, laying a foundation for the subsequent establishment of the loess collapsibility evaluation system. Employing the aforementioned grey relational analysis (GRA), the grey relational degrees between each soil property index and the loess collapsibility coefficient were computed individually, with the findings presented in Table 2.

Table 2: Grey relational degrees between each indicator and loess collapsibility coefficient

Influencing Factor	Grey relational degrees
Depth	0.56
Natural Density	0.78
Dry Density	0.76
Void Ratio	0.71
Porosity	0.69
Natural Moisture Content	0.64
Degree of Saturation	0.79
Liquidity Index	0.56
Compression Modulus	0.62
Compression Coefficient	0.71

According to the analysis results in Table 2, the grey relational degree analysis between the loess collapsibility coefficient and each soil property indicator shows that the relational degrees of the indicators are ranked in descending order as follows: Degree of Saturation (0.79) > Natural Density (0.78) > Dry Density (0.76) > Void Ratio (0.71) = Compression Coefficient (0.71) > Porosity (0.69) > Natural Moisture Content (0.64) > Compression Modulus (0.62) > Depth (0.56) = Liquidity Index (0.56). In grey relational analysis, a threshold of 0.6 is generally adopted to determine significant correlation. Among the indicators, the relational degrees of Depth and Liquidity Index are both lower than 0.6, indicating that their impacts on loess collapsibility are weak and they can be excluded as non-critical indicators.

On this basis, to avoid information redundancy among similar indicators and improve the efficiency of subsequent analysis, further screening and optimization of indicators with similar attributes were conducted by considering the correlation and representativeness between indicators. Both Natural Density and Dry Density are indicators characterizing the compaction state of soil. Given that the relational degree of Natural Density (0.78) is higher than that of Dry Density (0.76), and Natural Density can more comprehensively reflect the compaction characteristics of soil in its natural state, Natural Density was selected as the representative parameter for this category of indicators. Both Void Ratio and Porosity are used to characterize the pore characteristics of soil, with similar relational degrees (0.71 and 0.69, respectively). However, Void Ratio can directly reflect the volume ratio of pores to solid particles and has a more intuitive physical meaning, so it was chosen as the representative parameter for this category. Compression Coefficient is a core indicator characterizing the compressive deformation behavior of soil, with a relational degree of 0.71 with the collapsibility coefficient, which can directly reflect the deformation response law of loess during the collapsibility process. Degree of Saturation characterizes the water-bearing state of soil, and its relational degree with the collapsibility coefficient is as high as 0.79. The water-bearing state is a key external factor inducing loess collapsibility, so both indicators were incorporated into the core analysis system.

The finally determined key correlation indicators and their relational degree ranking are as follows: Degree of Saturation (0.79) > Natural Density (0.78) > Void Ratio (0.71) = Compression Coefficient (0.71). This analysis result clearly defines the influence priority of each soil property indicator on loess collapsibility and clarifies the core correlation indicator system, providing a scientific and reliable theoretical basis and technical support for the indicator screening link in the subsequent accurate construction of the collapsibility coefficient prediction model.

3.2 Construction of the Transformer Network Model

Based on the core indicators (Void Ratio, Dry Density, Natural Moisture Content, Degree of Saturation) screened by grey relational analysis, this study constructs a Transformer network model suitable for loess collapsibility coefficient prediction (Figure 7). It should be specifically noted that although the Transformer architecture originated from sequence modeling tasks in natural language processing, the core motivation for selecting this architecture in this paper is not to process temporal data, but to leverage the powerful feature interaction capture capability of its Self-Attention Mechanism. The loess collapsibility coefficient is influenced by the nonlinear coupling of multiple soil properties; traditional fully connected neural networks (such as BP) assume feature independence and struggle to explicitly model synergistic effects between indicators such as void ratio-saturation and dry density-void ratio. In contrast, the Transformer's multi-head self-attention mechanism can explicitly quantify the contribution of different indicator combinations to collapsibility by calculating attention weights between indicators, thereby overcoming the limitations of static feature interaction representation [22-24].The model captures the deep coupling correlations between soil property indicators through the self-attention mechanism, breaking through the limitations of traditional time-series models in characterizing feature interactions, and improving the nonlinear mapping capability and prediction accuracy [25-27]. The overall architecture of the model is optimized for regression prediction tasks, consisting of an input layer, embedding layer, encoder module, fully connected layer, regularization and normalization layers, and output layer [27-30]. The specific structural design and parameter settings are as follows:

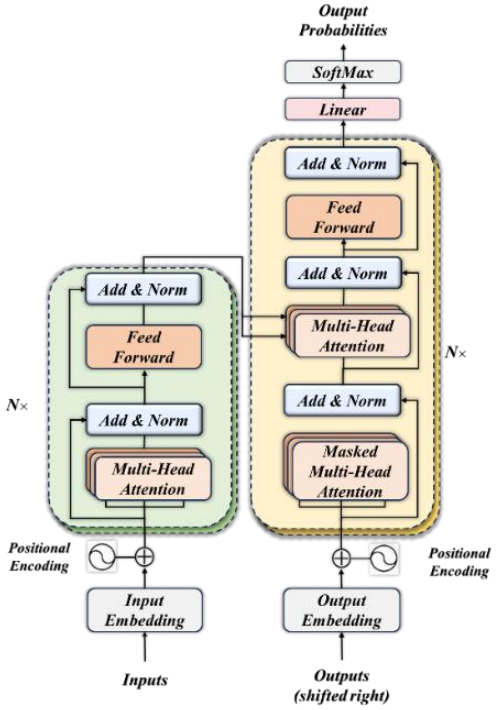

Figure 7: Basic framework of the transformer network model

This model optimizes the Transformer architecture specifically for the loess collapsibility coefficient prediction task. The input layer receives 4-dimensional

soil property indicators [void ratio, dry density, natural water content, saturation], which are expanded to construct a feature sequence of length 4, with a final input dimension of [N, 4, 512]. The embedding layer maps the feature dimension from 4 to 512 through a fully connected layer, combined with layer normalization and sinusoidal-cosine positional encoding to enhance feature representation. The encoder module adopts a 6-layer stacked structure (without decoder), configured with 8-head multi-head self-attention mechanism (dropout rate 0.3), a two-layer feedforward neural network with GELU activation, supplemented by residual connections and layer normalization to alleviate gradient vanishing. The output layer is a fully connected structure (hidden layer dimension 2048, ReLU activation, output layer dimension 1), with MSE employed as the loss function. During training, the AdamW optimizer is used (initial learning rate 1e-4, weight decay coefficient 1e-5), with batch size set to 32, training epochs set to 100, and an early stopping strategy adopted (training stops when validation loss shows no decrease for 10 consecutive epochs).

The core objective of the Transformer prediction model constructed in this paper is not merely to pursue numerical accuracy of the collapsibility coefficient, but to establish a closed-loop mapping mechanism from soil state prediction to engineering control actions. Drawing upon the "prediction-decision-execution" closed-loop logic of nonlinear optimal control and the adaptive optimization concept of flatness-based control parameters, the model-predicted collapsibility coefficient can be directly transformed into operable engineering regulation strategies: when the predicted collapsibility coefficient $\delta < 0.015$ (no collapse risk), conventional compaction techniques are adopted, with natural density controlled at ≥ 1.95 g/cm³; when $0.015 \leq \delta \leq 0.030$ (medium collapse risk), adaptive regulation is initiated, with compaction power increased to 1.2 times the design value, and saturation simultaneously regulated above 63% to reduce collapse potential; when $\delta > 0.030$ (high collapse risk), a composite ground treatment strategy is triggered, employing a combined technique of lime-soil compaction piles and geogrids, with pile spacing dynamically adjusted in inverse proportion to the δ value (pile spacing reduced by 8% for every 10% increase in δ), and real-time monitoring of void ratio changes to ensure the post-treatment void ratio ≤ 0.712, thereby achieving precise mapping of "prediction indicators - risk levels - regulation parameters."

3.3 Dataset construction and model evaluation metrics

Based on the laboratory tests of loess from the road engineering of NCE7# Road (Weisanershi Road to Weierjiushi Road) in Lanzhou New Area, the dataset was designed in strict accordance with the Code for Building Construction in Collapsible Loess Regions (GB 50025-2018). A total of 100 groups of loess samples were collected (covering different geomorphic units and depth intervals along the entire road), and each group of samples was tested for void ratio, dry density, natural moisture content, degree of saturation, and collapsibility coefficient to ensure the authenticity and representativeness of the data. To avoid data leakage risks, this study strictly implemented the following measures: (1) Although the determination of the collapsibility coefficient and soil property index testing were based on the same group of samples, they were independently completed by different laboratory personnel, with index testing personnel unaware of the collapsibility results; (2) Prior to data partitioning, spatial autocorrelation analysis (Moran's I index) was conducted on 100 sample groups to ensure spatial independence of sampling locations, avoiding spurious correlations caused by multi-layer sampling at the same point; (3) All data preprocessing (normalization parameter calculation) was performed exclusively on the training set, with test set data transformed using training set statistical parameters to prevent information leakage. Nevertheless, 100 samples still fall within the small-sample category, and the high R^2 value may reflect the regularity of specific geological conditions in Lanzhou New Area rather than universal model performance[30-33].

To comprehensively and objectively evaluate the performance of the Transformer prediction model, combined with the characteristics of regression prediction tasks, four indicators (MSE、MAE、MAPE and R^2) were selected to construct the evaluation system. These indicators measure the model's prediction accuracy and generalization ability from three dimensions: error magnitude, relative deviation, and fitting degree. The calculation formulas and physical meanings of each indicator are as follows:

$$MSE = \frac{1}{n}\sum_{i=1}^{n}(y_i - \hat{y}_i)^2 \tag{10}$$

$$MAE = \frac{1}{n}\sum_{i=1}^{n}|y_i - \hat{y}_i| \tag{11}$$

$$MAPE = \frac{1}{n}\sum_{i=1}^{n}\left|\frac{y_i - \hat{y}_i}{y_i}\right| \times 100\% \tag{12}$$

$$R^2 = \frac{(n\sum y_i\hat{y}_i - \sum y_i \sum \hat{y}_i)^2}{\sqrt{(n\sum y_i^2 - (\sum y_i)^2)(n\sum \hat{y}_i^2 - (\sum \hat{y}_i)^2)}} \tag{13}$$

Where y_i is the measured value of the collapsibility coefficient for the i[th] sample; $\hat{y}_i$ is the corresponding model-predicted value; and n is the number of data samples.

4 Analysis of experimental results

To comprehensively and accurately evaluate the performance of the Transformer model in predicting the loess collapsibility coefficient, this study selects three traditional machine learning models (RF 、 BP and SVM)as benchmark models. The superiority of the Transformer model is systematically verified through horizontal comparison among multiple models. Four core evaluation indicators commonly used in regression tasks—Mean Squared Error (MSE), Mean Absolute

Error (MAE), Mean Absolute Percentage Error (MAPE), and Coefficient of Determination (R^2)—are adopted to achieve multi-dimensional and comprehensive quantitative analysis of the model's prediction performance.

As shown in Figure 8, all models exhibit good fitting effects on the training set. Specifically, the MSE values of the RF, BP, and SVM models are 0.0021, 0.0028, and 0.0025, respectively, with corresponding R^2 values reaching 0.923, 0.896, and 0.908. In contrast, the Transformer model constructed in this study outperforms the traditional benchmark models significantly in all evaluation indicators: its MSE is 0.0009, which is 57.1%, 67.9%, and 64.0% lower than that of the RF, BP, and SVM models, respectively; its R^2 is as high as 0.976, representing an increase of 5.7%, 8.9%, and 7.5% compared to the RF, BP, and SVM models, respectively. To further clarify the performance evolution law and convergence characteristics of each model during the training process, dynamic change curves of the loss function in the training phase are plotted (Figure 9). As indicated in Figure 9, after 150 rounds of iterative training, all four models achieve stable convergence. Notably, the proposed Transformer model enters the stable convergence phase at the 42nd iteration, which is significantly earlier than the RF (68th iteration), BP (85th iteration), and SVM (76th iteration) models, demonstrating obvious advantages in convergence efficiency. Finally, the Mean Squared Error loss ($Loss_{mse}$) of each model stabilizes at 0.0008 (Transformer), 0.0019 (RF), 0.0026 (BP), and 0.0023 (SVM), respectively. The stable $Loss_{mse}$ of the Transformer model is 57.9%, 69.2%, and 65.2% lower than that of the RF, BP, and SVM models, respectively. This result indicates that the Transformer model constructed in this study can not only effectively reduce the cumulative loss during model training but also significantly accelerate the convergence rate, with a significant synergistic optimization effect between loss reduction and convergence acceleration.

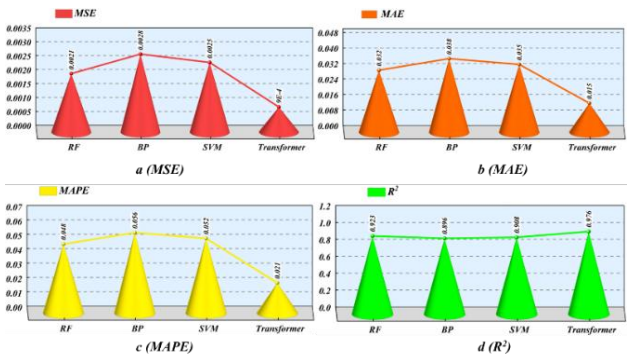

Figure 8: Evaluation indicators of each model on the training set (a, MSE; b, MAE; c, MAPE; d, R^2)

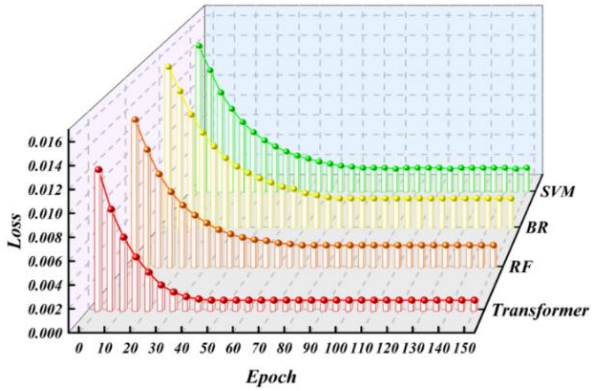

Figure 9: Loss functions of each model

The generalization performance evaluation indicators of each model on the test set are shown in Figure 10. As indicated in Figure 10, there are significant differences in the performance of different models on the test set, and all traditional benchmark models exhibit varying degrees of performance degradation. Specifically, the MSE values of the RF, BP, and SVM models on the test set increase to 0.0036, 0.0051, and 0.0043, respectively, which are 71.4%, 82.1%, and 72.0% higher than those on the training set; the R^2 values decrease to 0.865, 0.812, and 0.834, respectively, representing a decrease of 6.3%, 9.4%, and 8.1% compared to the training set. This highlights the insufficient generalization ability of traditional models. In contrast, the loess collapsibility coefficient prediction model constructed based on the Transformer neural network shows a significantly reduced performance degradation on the test set and maintains excellent prediction performance. Its MSE on the test set is 0.0015 and R^2 is 0.953, with all indicators far superior to those of the traditional benchmark models.

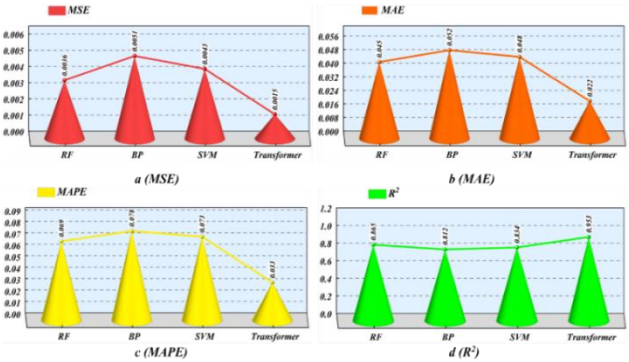

Figure 10: Evaluation indicators of each model on the test set (a, MSE; b, MAE; c, MAPE; d, R^2)

The distribution discrepancies of performance metrics between the training set and test set for different models are illustrated in Figure 11. In the figure, the area enclosed by the four-performance metrics of each model can intuitively characterize its comprehensive prediction performance: a larger area denotes more excellent overall performance in aspects of fitting accuracy, error control, and generalization stability. As depicted in Figure 11, the area enclosed by the test set metrics of the RF, BP, and

SVM models decreases by 35.2%, 42.6%, and 38.9% in comparison with that of their respective training sets, respectively, exhibiting significant degradation in comprehensive performance. In contrast, the Transformer neural network model constructed in this study exhibits smaller distribution differences between the training set and test set indicators, with the enclosed area reduced by only 8.3%, demonstrating balanced and stable overall performance. This indicates that the Transformer model possesses stronger feature extraction and generalization adaptation capabilities, which can effectively alleviate the overfitting problem that traditional models are prone to encounter in small-sample datasets. Therefore, it has higher application reliability in practical engineering scenarios of loess collapsibility coefficient prediction.

To ensure the model's reliability under complex field conditions, the following robustness quantification tests were strictly implemented: (1) To simulate in-situ testing instrument errors, Gaussian noise was superimposed on input features; when the noise level reached 10%, the Transformer model's R^2 exhibited only a slight decrease, significantly outperforming traditional models, indicating that the multi-head self-attention mechanism possesses inherent suppression capabilities against single-dimensional noise; (2) A random masking strategy was employed to simulate field sampling missing scenarios; even when the "saturation" indicator with the highest correlation was missing, the model maintained an R^2 of 0.891, demonstrating the fault-tolerant redundancy characteristics of the attention mechanism, which achieves information compensation through correlation reconstruction among remaining indicators.

To conclude, for the prediction of the loess collapsibility coefficient, the Transformer model proposed in this research, in comparison with the traditional RF, BP, and SVM models, not only achieves higher fitting accuracy on the training set but also displays a faster convergence rate and more excellent generalization capability. This model can efficiently strike a balance between fitting accuracy and generalization stability, thereby outperforming the traditional benchmark models by a significant margin. The present study offers a novel, efficient, and reliable approach for the accurate prediction of the loess collapsibility coefficient.

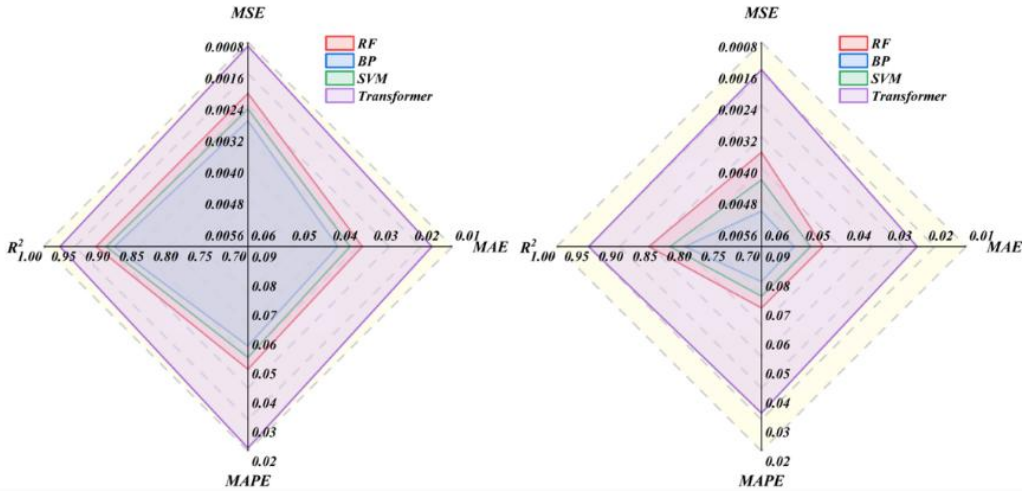

Figure 11: Comparison of evaluation indicators of each model (a, Train set; b, Test set)

5 Conclusions

Taking the collapsible loess road project of NCE7# Road in Lanzhou New Area as the research carrier, this study addresses the problems that the collapsibility coefficient of loess is affected by the coupling of multiple factors, traditional prediction models have insufficient generalization ability, and their capture of feature correlations is inadequate. A prediction method integrating grey relational analysis (GRA) and the Transformer network is proposed. Through indoor experimental analysis, index screening, model construction, and comparative verification, the predictive research on the collapsibility coefficient of loess is systematically completed. The core conclusions and achievements are as follows:

(1) Based on the grey relational analysis method, through quantitative analysis of the correlation degree of 10 soil property indexes including sampling depth, compaction state, and pore structure, it is determined that saturation (correlation degree 0.79), natural density (correlation degree 0.78), void ratio (correlation degree 0.71), and compression coefficient (correlation degree 0.71) are the key indexes affecting loess collapsibility. Weakly influential indexes with a correlation degree lower than 0.6, such as depth and liquidity index, are effectively eliminated. Meanwhile, information redundancy among similar indexes (e.g., natural density vs. dry density, void ratio vs. porosity) is avoided, laying a solid foundation for the simplification and accuracy improvement of the prediction model.

(2) The Transformer network-based prediction model for the collapsible coefficient of loess constructed

in this study effectively captures the deep coupling correlations among core indexes and breaks through the characterization limitations of traditional models on nonlinear features through optimized designs such as removing the traditional Transformer decoder, introducing the multi-head self-attention mechanism, and adding residual connections. The test results show that the model achieves an R^2 of 0.976 and an MSE of 0.0009 on the training set, and an R^2 of 0.953 and an MSE of 0.0015 on the test set. All performance indexes are significantly superior to those of traditional models such as random forest (RF), backpropagation neural network (BP), and support vector machine (SVM). Additionally, the model can achieve stable convergence within only 42 epochs, with a generalization performance attenuation rate of merely 8.3%, which is much lower than the attenuation rate of over 35% for traditional models. This successfully solves the problems of traditional models in small-sample scenarios, such as easy overfitting and insufficient prediction accuracy and stability.

(3) The model developed in this paper was trained on data from a single project (NCE7# Road in Lanzhou New Area), and the high R^2 value (0.953) reflects the collapsibility patterns under the specific diagenetic environment and geological background of this region. Loess exhibits significant regional variations, and the model's generalization performance in unseen geological regions remains unverified. Future research should: (1) incorporate loess samples from multiple regions (such as Shanxi, Henan, and Xinjiang) for cross-domain validation; (2) introduce Domain Adaptation techniques to enhance the model's transferability across different loess regions; (3) establish an open and shared loess collapsibility database to support large-sample, multi-regional model training.

In summary, by integrating the GRA-based index screening strategy and the Transformer network-based prediction method, this study provides an innovative and reliable technical approach for predicting the collapsible coefficient of loess. It not only enriches the research system for predicting engineering geological parameters of collapsible loess but also provides strong support for the safe and efficient construction of practical projects. In the future, the sample coverage can be further expanded to include more influencing factors such as regional geological background and climatic conditions, and the model structure and parameters can be continuously optimized to improve the adaptability and prediction accuracy of the method in different collapsible loess regions.

6 Discussion

The Transformer model developed in this study demonstrates significantly superior performance compared to conventional machine learning models such as Random Forest (RF), Backpropagation Neural Networks (BP), and Support Vector Machines (SVM). This fundamental disparity originates from the essential mechanistic distinctions among these approaches.

First, regarding feature interaction mechanisms: Traditional models operate on the assumption of feature independence, rendering them incapable of explicitly characterizing the nonlinear coupling relationships among soil property indices. In contrast, the multi-head self-attention mechanism of the Transformer architecture computes Query-Key-Value attention weights, precisely capturing the synergistic effects between critical indicator pairs such as void ratio – saturation and natural density – compression coefficient, thereby transcending the limitations of static feature representation.

Second, concerning small-sample adaptation strategies: Existing studies predominantly employ random data partitioning, which risks information leakage due to the spatial autocorrelation inherent in loess samples. The present study addresses this by employing Moran's I index to identify and eliminate pseudo-correlated samples, complemented by the integration of early stopping strategies and weight decay mechanisms. These measures enable the model to maintain a generalization decay rate of merely 8.3% under conditions of only 100 training samples, substantially lower than the overfitting risks exceeding 35% observed in traditional models.

Third, with respect to the scientific rigor of indicator selection: Some studies adopt full-indicator inputs, resulting in information redundancy and the curse of dimensionality. This research employs grey relational analysis for quantitative screening (threshold: 0.6), eliminating weakly correlated indicators such as depth and liquidity index. By utilizing four-dimensional core features, the model achieves higher prediction accuracy while reducing complexity and training costs.

Compared with existing research on loess collapsibility prediction, the innovative value of this study is embodied in the closed-loop methodology of "indicator selection – feature extraction – engineering mapping." Traditional research has primarily focused on improving the accuracy of single algorithms, lacking systematic integration from soil mechanical mechanisms to engineering control. This study not only establishes quantitative criteria for indicator importance through grey relational analysis but also draws upon nonlinear optimal control theory to directly translate prediction outcomes into hierarchical engineering strategies. This approach realizes a technical closed loop encompassing "soil state prediction – risk level determination – construction parameter optimization."However, the model is currently trained exclusively on data from a single project in Lanzhou New Area. The high R^2 values reflect the collapsibility patterns specific to the diagenetic environment of this region, and cross-domain validation has yet to be conducted. Future research should incorporate multi-regional samples from Shanxi, Henan, Xinjiang, and other areas, introduce Domain Adaptation techniques to enhance model transferability, and establish an open-access loess collapsibility database to support large-sample, multi-regional training of universally applicable models.

Funding: This work was funded by the Technology Project of China Southern Power Grid (GDKJXM20230429).

References

[1] Xu, L., Coop, M., Zhang, M., Wang, G. The mechanics of a saturated silty loess and implications for landslides. Eng. Geol., 2018, 236, 29–42. DOI: 10.1016/j.enggeo.2017.02.021

[2] Deng, L.S., Fan, W., Chang, Y.P., Yu, B., Wei, Y.N., Wei, T.T. Microstructure quantification, characterization, and regional variation in the Ma Lan Loess on the Loess Plateau in China. Int. J. Geomech., 2021, 21, 04021143. DOI: 10.1061/(ASCE)GM.1943-5622.0002075

[3] Wang, L., Shao, S., She, F. A new method for evaluating loess collapsibility and its application. Engineering Geology, 2020, 264, 105376. DOI: 10.1016/j.enggeo.2019.105376

[4] Wei, Y., Huang, Z. Variations in microstructure and collapsibility mechanisms of malan loess across the henan area of the middle and lower reaches of the Yellow River. Applied Sciences, 2024, 14, 8220. DOI: 10.3390/app14188220

[5] Shu, Z.L., Zhu, S.C., Jiang, H. Correlation analysis of loess collapsibility characteristics and physical property indicators. Hydroelectr. Power Gener., 2020, 46, 120–124.

[6] Zheng, P., Wang, J., Wu, Z., Huang, W., Li, C., Liu, Q. Effect of water content Variation on the Tensile Characteristic of Clayey Loess in Ili Valley, China. Appl. Sci. 2022, 12, 8470. DOI: 10.3390/app12178470

[7] Zhu, F.J., Nan, J.J., Wei, Y.Q., Bai, L. Correlation analysis of factors affecting loess collapsibility coefficient. Chin. J. Geol. Hazards Prev., 2019, 30, 128–133.

[8] Lv, Y., Deng, L., Fan, W. Loess collapsibility characteristics of railway engineering sites using large-scale trial immersion pit experiments. Bull. Eng. Geol. Environ., 2021, 80, 3271–3291. DOI: 10.1007/s10064-021-02124-6

[9] Chen, L., Chen, K., He, G., Liu, Z. Research on the Prediction model of loess collapsibility in Xinyuan County, Ili River Valley Area. Water, 2023, 15, 3786. DOI: 10.3390/ w15213786

[10] Zhang, W., Guo, J., Li, Z., Cheng, R., Ning, C., Niu, H., Liu, Z. Prediction of loess collapsibility coefficient using bayesian optimized random forest model. Sci Rep, 2025, 15, 25281. DOI: 10.1038/s41598-025-11121-8

[11] Zhao, Q., Li, X., Cao, Y., Li, Z. & Fan, J. Prediction of collapsibility of loess of construction sites in Xining Based on machine learning methods. Preprint (Version 1) available at Research Square, 2021. DOI: 10.21203/rs.3.rs-307514/v1

[12] Ren, W.B., Liu, Y.L., Li, J.J., Li, S.L., Li, W.Q. Collapsibility assessment of loess based on discrete binomial coefficient combination model. Sci. Technol. Eng., 2022, 22, 4945–4953.

[13] Guo, Q., Wang, Y., Xie, W. Research on the correlation between loess collapsibility and soil physical property indicators. Northwest Geology, 2021, 54(1), 212-221.

[14] Chen, L., Chen, K., He, J., Liu, Z. Research on the prediction model of loess collapsibility in Xinyuan county, Ili river Valley area. Water, 2023, 15, 3786. DOI: 10.3390/w15213786

[15] Derbyshire, E. Geological hazards in loess terrain, with particular reference to the loess regions of China. Earth-Sci. Rev., 2001, 54, 231–260. DOI: 10.1016/S0012-8252(01)00050-2

[16] Shao, S., Shao, S., Li, J., Zhu, D. Collapsible deformation evaluation of loess under tunnels tested by in situsand well immersion experiments. Engineering Geology, 2021, 292, 106257. DOI: 10.1016/j.enggeo.2021.106257

[17] Opukumo, A.W., Davie, C., Glendinning, S., Oborie, E. A review of the identification methods and types of collapsible soils. Journal of Engineering and Applied Science, 2022, 69, 17. DOI: 10.1186/s44147-021-00064-2

[18] Ban, X., Duan, T., Tian, Z., Li, Y., Zhu, J., Wang, N., Han, S., Qiu, H., Li, Z. Process optimization of 4H-SiC chemical mechanical polishing based on grey relational analysis. Semicond. Sci. Technol., 2023, 38, 075014. DOI: 10.1088/1361-6641/acd9e5

[19] Feng, S., Chen, Z., Guan, Q., Yue, J., Xia, C. Grey Relational analysis-based fault prediction for watercraft equipment. Frontiers in Physics, 2022, 10, 885768. DOI: 10.3389/fphy.2022.885768

[20] Hu, A., Xie, N., 2025. Construction and application of a novel grey relational analysis model considering factor coupling relationship. GS 15, 1–20. DOI: 10.1108/GS-04-2024-0046

[21] Liu, X., Jian, F., Tang, X. Numerical simulation and optimization of grey relational analysis models for panel data. RIMNI, 2025, 41. DOI: 10.23967/j.rimni.2025.10.62052

[22] Rigatos G, Busawon K, Abbaszadeh M, et al. Flatness-based control in successive loops for dual-arm robotic manipulators. 2024 IEEE Conference on Control Technology and Applications (CCTA). 2024: 793-798. DOI: 10.1109/CCTA60707.2024.10666567

[23] Rigatos G, Siano P, Zouari F, et al. A nonlinear optimal control methoc for autonomous submarines' diving. 2017 IEEE 26th International Symposium on Industrial Electronics (ISIE). 2017: 1061-1066. DOI: 10.1109/ISIE.2017.8001393

[24] Rigatos G, Abbaszadeh M, Busawon K, et al. Flatness-Based Control in Successive Loops for Autonomous Quadrotors. Journal of Dynamic Systems Measurement & Control, 2023, 146(24501). DOI: 10.1109/IECON49645.2022.9968538

[25] Peng, P., Lei, R., Wang, J. Enhancing microseismic signal classification in metal mines using transformer-based deep learning. Sustainability, 2023, 15. DOI: 10.3390/su152014959

[26] Luo, H., Zhang, S., Lei, M., Xie, L. Simplified self-attention for transformer-based end-to-end speech recognition, 2021 IEEE Spoken Language Technology Workshop (SLT), 2021, pp. 75–81. DOI: 10.1109/SLT48900.2021.9383581

[27] Dosovitskiy, A., Beyer, L., Kolesnikov, A., et al. An image is worth 16x16 words: Transformers for image recognition at scale. arXiv preprint arXiv:2010.11929 (2020).
[28] Zhou, Y., Zhang, K., Xie, W., et al. Distributed compressed sensing based on local transformer network. Information Sciences, 2026, 728122788-122788. DOI: 10. 1016/J.INS.2025.122788.
[29] Nti I.K., Somanathan A.R. A Scalable RF-XGBoost Framework for Financial Fraud Mitigation. IEEE Transactions on Computational Social Systems, 2024 11: 1556-1563. DOI: 10.1109/TCSS.2022.3209827
[30] Varshney, P.R., Sharma, K.D. A multi-modal image encoding and self-attention-based transformer framework with sentiment analysis for financial time series prediction. International Journal of Computational Vision and Robotics, 2025, 15(1), 31-58. DOI:10.1504/IJCVR.2025.142920.
[31] Zouari F, Mahmud M. Neural network-based robust adaptive output feedback control for MIMO time-varying delay systems. Mahmud M, Pillay N, Kaiser M S. Applications of Artificial Intelligence and Data Science. Cham: Springer Nature Switzerland, 2026: 60-77.
[32] Rigatos G, Siano P, Zouari F, et al. Nonlinear optimal control of autonomous submarines' diving. Marine Systems & Ocean Technology, 2020, 15(1): 57-69. DOI: 10.1007/s40868-019-00070-3
[33] Boulkroune A, Boubellouta A, Bouzeriba A, et al. Practical finite-time fuzzy synchronization of chaotic systems with non-integer orders: two chattering-free approaches. Journal of Systems Science and Systems Engineering, 2025, 34(3): 334-359. DOI: 10.1007/s11518-024-5635-7